ARMY RESEARCH LABORATORY

Stefan Model of the Post-transition Plasma Environment Encountered in Solid Armature Railguns

by Andrew J. Porwitzky

ARL-TR-5112 **March 2010**

NOTICES

Disclaimers

The findings in this report are not to be construed as an official Department of the Army position unless so designated by other authorized documents.

Citation of manufacturer's or trade names does not constitute an official endorsement or approval of the use thereof.

Destroy this report when it is no longer needed. Do not return it to the originator.

Army Research Laboratory
Aberdeen Proving Ground, MD 21005-5069

ARL-TR-5112 **March 2010**

Stefan Model of the Post-transition Plasma Environment Encountered in Solid Armature Railguns

Andrew J. Porwitzky
Weapons and Materials Research Directorate, ARL

REPORT DOCUMENTATION PAGE	Form Approved OMB No. 0704-0188

1. REPORT DATE *(DD-MM-YYYY)*	2. REPORT TYPE	3. DATES COVERED (From - To)
March 2010	Final	

4. TITLE AND SUBTITLE	5a. CONTRACT NUMBER
Stefan Model of the Post-transition Plasma Environment Encountered in Solid Armature Railguns	5b. GRANT NUMBER
	5c. PROGRAM ELEMENT NUMBER

6. AUTHOR(S)	5d. PROJECT NUMBER
Andrew J. Porwitzky	5e. TASK NUMBER
	5f. WORK UNIT NUMBER

7. PERFORMING ORGANIZATION NAME(S) AND ADDRESS(ES)	8. PERFORMING ORGANIZATION REPORT NUMBER
U.S. Army Research Laboratory ATTN: RDRL-WMP-A Aberdeen Proving Ground, MD 21005	ARL-TR-5112

9. SPONSORING/MONITORING AGENCY NAME(S) AND ADDRESS(ES)	10. SPONSOR/MONITOR'S ACRONYM(S)
	11. SPONSOR/MONITOR'S REPORT NUMBER(S)

12. DISTRIBUTION/AVAILABILITY STATEMENT

Approved for public release; distribution unlimited.

13. SUPPLEMENTARY NOTES

14. ABSTRACT

Presented is a model for plasma generation in the post-transition interface for solid armature railguns. The model assumes that the plasma in the post-transition interface is generated by vaporization of armature material via thermal contact with the high temperature plasma, which is maintaining electrical conductivity. The model indicates that it is possible to generate sufficiently high mass loss rates from this method under the existing experimental conditions. However, the model results in armature wear patterns that are contradictory to what is seen in experiments. A brief look forward to arcing contact ablation models and the unique difficulties they face is also presented.

15. SUBJECT TERMS

Railguns, Stefan, plasma, transition, modeling

16. SECURITY CLASSIFICATION OF:			17. LIMITATION OF ABSTRACT	18. NUMBER OF PAGES	19a. NAME OF RESPONSIBLE PERSON
a. REPORT	b. ABSTRACT	c. THIS PAGE			Andrew J. Porwitzky
Unclassified	Unclassified	Unclassified	UU	22	19b. TELEPHONE NUMBER (*Include area code*) (410) 278-9875

Standard Form 298 (Rev. 8/98)
Prescribed by ANSI Std. Z39.18

Contents

List of Figures

List of Tables

Acknowledgments

The author would like to thank Dr. John Powell and Mr. Alex Zielinski for many useful discussions in relation to the present work.

INTENTIONALLY LEFT BLANK.

1. Introduction

High velocity (defined here as having an exit velocity of approximately 2000 m/s) solid armature railguns frequently undergo a change in armature-rail electrical contact commonly referred to as "transition". A post-transition environment is characterized by enhanced rail damage and a drastic increase in the rail voltage (Abrams et al., 2007). The increase in rail voltage is consistent with a contact resistivity on the order of typical plasma resistivities (Abrams et al., 2007). It is thus generally accepted that transition indicates the point at which the electrical contact "transitions" from either solid or liquid contact (depending on the specific conditions pre-transition) to plasma contact. It is also generally accepted that this plasma must come from arc discharge, although no quantitative justification of this can be found, nor are there any detailed models for arcing contact in solid armature railguns. The present paper investigates an alternative possibility for plasma generation in the armature-rail interface, namely, thermal vaporization of armature material. The model will attempt to address whether or not this mechanism can account for the amount of armature material lost in the post-transition environment.

The difference between "arc plasma" and "thermally vaporized plasma" may not be obvious. Although nearly identical in composition, the mechanism of their generation is key to the problem at hand. A thermally vaporized plasma is generated by the phase transition from solid to liquid, to vapor and finally plasma. This transition happens due simply to the presence of a high temperature source heating the plasma source material. In the present model it is assumed that the high temperature source is a plasma already in existence, the source of which can be debated, but is not of critical importance here now. It may come from an initial arcing, or from a gaseous hot spot, or simply from Joule heating of a weekly conductive vapor.

Plasma generation by means of an electric arc is a very different phenomenon. Electric arcs involve cathode and anode spots which leave distinct surface features on their respective surfaces, which themselves contribute to ablative material loss, entirely independent of the arc. The arc itself is a highly localized, high temperature plasma which causes physical damage to the contact surfaces (known as ablation) that is entirely separate from thermal vaporization (Boxman, 1995). The simplest way to conceptualize the differences between arcing and vaporization as plasma generation mechanisms is that arcing is an extremely complex and violent process, while thermal vaporization is comparatively simple and predictable.

Although there has been progress in recent years with technology to delay transition, it appears that transition will always occur for high velocity railguns, albeit for a short distance. Note that any contact transition yields significant rail damage and contributes to decreasing the operational lifetime of the launcher (Zielinski and Denny, 2009).

2. Overview of Stefan & Interface Model

The physical configuration of the post-transition interface is taken to be as follows. There exists a gap in the rail-armature interface that is filled with plasma. The plasma is composed of vaporized armature material, taken here to be atomic aluminum; the possibility of plasma generated by ionized air is neglected. According to melt-wave theory, the interface condition just prior to transition involves the current flowing through a liquid contact environment (Barber et al., 2003). Thus, it is assumed that the armature surface is in a liquid state. The geometry adopted is shown in figure 1. Any boundary layer effect or heat flux to the rails is neglected in the present model, as is the motion of the rails.

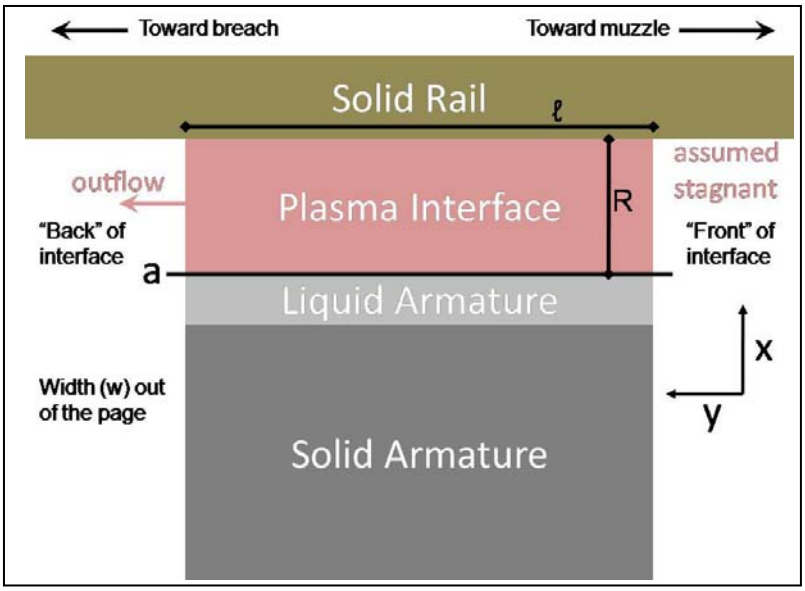

Figure 1. Model geometry (not to scale).

The method of Stefan is used to model this problem. A Stefan problem is essentially a heat transfer problem with an additional constraint equation (Crank, 1987). The Stefan condition accounts for phase transition of the heating surface, and determines the rate at which the surface recedes. Stefan originally developed this condition for modeling the melting of glaciers in seawater. In that case, the Stefan condition is applied at the ice/seawater interface and determines the rate at which the surface of the ice recedes. For the present application, the liquid-plasma interface, which is labeled as *a* in figure 1, is to be tracked. The solid-liquid interface recedes slowly compared to the recession of interface *a*. Thus, the Stefan problem is represented as a single phase model of the liquid armature. The Stefan condition at *a* is given as equation 1.

$$\left(e + \frac{p}{\rho}\right)\rho_{liq}\frac{da}{dt} = -K\frac{dT_l}{dx} - \sigma_B T^4 \tag{1}$$

The Stefan condition is a form of the energy conservation equation at the liquid-plasma interface. The first term represents the energy absorbed to move interface *a* via vaporization at the rate da/dt. The second term is the energy exiting the interface by thermal diffusion into the liquid, where T_l is the temperature in the liquid armature at *a*, and K is the thermal conductivity of liquid aluminum. The third term is energy added to the interface via black body radiation from the plasma. The remaining variables in equation 1 are defined as follows: e is the specific internal energy of the gas, which includes translational, heat of vaporization, and the first three ionization levels. Gas pressure in the interface is given as p, while gas mass density is ρ. ρ_{liq}=2294 kg/m^3 is the mass density of liquid aluminum, σ_B is the Stefan-Boltzmann constant, and T is the steady state plasma temperature in the interface.

Initially, equation 1 was solved computationally. However, it was found that the temperature gradient at *a* is extremely small in relation to the other terms. Neglecting the temperature gradient allows for the analytical solution of equation 1, given as equation 2. An analytical solution yields much more physical insight. This result can also be used directly in the fluid model presented below. Note that $(e + \frac{p}{\rho})$ is itself a function of *T*.

$$\left|\frac{da}{dt}\right| = \frac{\sigma_B T^4}{(e+\frac{p}{\rho})\,\rho_{liq}} \tag{2}$$

The model for the plasma in the interface is inspired by Powell's model for ETC capillaries (Powell et al., 1992). The simplified mass, momentum, and energy conservation equations are solved in the plasma interface, given assumptions of the state of the plasma at the front and back of the interface. It is assumed that the plasma flows out the interface at the back of the armature (at $y = l$) at the isothermal sound speed due to the plasma pressure in the interface (choked flow), namely, $v_l = \sqrt{\frac{k\,T}{m}}$, where k is Boltzmann's constant, and m is the mass of an aluminum ion. At the front end of the interface, the plasma velocity is assumed to be zero. This is not an entirely physical assumption, but allows for the solution of the conservation equations involving only one fluid. If inflow velocity were taken into account, a two fluid model would have to be used as the incoming fluid would be the ambient atmosphere. This ambient inflow would mix with the plasma in the interface, dropping the temperature and resulting in a decreased surface recession rate. The results of using this assumption thus generate the largest surface recession rate possible under the theoretical framework of a vaporizing armature.

The gas pressure and density are related by the expression $p = \rho {v_l}^2$. The steady state, isothermal mass, momentum and energy conservation equations, under the assumptions listed previously, reduce to the expressions given as equations 3, 4 and 5, respectively. The subscript "0" denotes values at the leading (stagnant) edge of the plasma interface, while subscript l denotes values at the outflow of the plasma interface (Powell et al., 1992).

$$\rho_l = \frac{\Gamma\, l}{v_l} \tag{3}$$

$$\rho_0 = 2\frac{\Gamma\, l}{v_l} \tag{4}$$

$$\rho_l E_l v_l = \frac{I^2}{\sigma\, w^2 l} - \rho_l {v_l}^3 \tag{5}$$

The energy conservation expression (equation 5) must be solved numerically for T after the expressions for v_l and e are inserted. Included in equation 5 is Joule heating of the plasma column, where I is the total electric current through the column, σ is the plasma electrical conductivity, and w is the width of the contact region. The ablation rate is defined in terms of the recession rate of the liquid-plasma interface as

$$\Gamma = \frac{\rho_{liq}}{R}\frac{da}{dt}, \tag{6}$$

where R is defined in figure 1 as the height of the liquid armature-rail gap. This is synonymous with the height of the plasma column in the model.

The total internal energy at the outlet is expressed as $E_l = e + v_l^2/2$, where e is the specific internal energy of the gas in the interface, which includes ionization effects via Saha equilibrium (Powell, 1992). The specific internal energy is thus

$$e = L_v + \frac{3\,k}{2\,m}T(1+\alpha_e) + \frac{I_1}{m}\alpha_1 + \frac{I_1+I_2}{m}\alpha_2 + \frac{I_1+I_2+I_3}{m}\alpha_3\,, \tag{7}$$

where L_v=1.09x10^7 J/kg is the heat of vaporization of liquid aluminum, α_i is the ionization fraction for the i^{th} ionization level, and $i \in [1,3]$. The electron fraction is defined as $\alpha_e = \alpha_1 + 2\alpha_2 + 3\alpha_3$, and obviously $1 = \alpha_0 + \alpha_1 + \alpha_2 + \alpha_3$. The ionization potentials, I_i, for the first three ionization levels of atomic aluminum are listed in table 1. It is assumed that the electron excitation energy is negligible, which is generally true when the plasma will exist in multiple ionized states.

Table 1. Ionization potentials and degeneracies for atomic aluminum.

i	I_i	g_i
0	—	1
1	5.984 eV	2
2	18.823 eV	1
3	28.440 eV	2

The ionization fractions are defined by the Saha equation,

$$\frac{\alpha_{j+1}\,\alpha_e}{\alpha_j} = \frac{2m}{\rho_l}\frac{g_{j+1}}{g_j}\left(\frac{2\pi m_e kT}{h^2}\right)^{3/2}\mathrm{Exp}\left(\frac{-I_{j+1}}{kT}\right),\ j \in [0,2]. \tag{8}$$

Due to the analytical solution to the Stefan problem, the model reduces to numerically solving equations 5 and 8, noting that equation 8 is itself a set of three coupled equations. This is achieved using a multivariable root finding algorithm in the commercial software Mathematica.

The variables solved for directly are the plasma temperature and the three ionization fractions, α_1, α_2, and α_3, while da/dt is determined from equation 2.

Although not used in the present calculations, note that it is possible to reduce the above system of equations (equations 2, 3, 5, and 6) to a very simple solution for the plasma temperature by neglecting the kinetic energy of the gas with regard to its internal energy. Under this assumption, the exact form of the specific internal energy (equation 7) drops out and we are left with

$$T^4 = \frac{I^2 R}{w^2 l^2 \sigma \sigma_B}, \tag{9}$$

which is similar in form to the result obtained in Powell et al., 1992, but for non-cylindrical geometry. If equation 9 is used, then only equation 8 needs to be solved computationally.

3. Results & Implications

For the calculations contained in this report, the plasma in the post-transition interface is assumed to be composed of atomic aluminum generated by armature vaporization, thus m=13 amu. The electrical conductivity was chosen as a typical order of magnitude estimate for plasma conductivity, specifically σ=10^4 S/m (Marshall, 1986). The remaining parameters are estimated from the two-dimensional armature model developed by Powell et al., 2005. The total electrical current, length and width of the interface that carries the current are estimated to be I=6×10^5 A (Zielinski and Denny, 2009), l=5 mm (Powell et al., 2005), and w=2 cm (total width of armature via author's measurements) respectively. A range for the thickness of the plasma filled gap is used, with the maximum taken to be R=1.0 mm. Shown in figure 2 are photographs of the sample armature referenced for physical dimensions. This armature was part of an experimental sequence presented in Zielinski and Denny, 2009. Note that there is significant preferential corner erosion and a sharpening of the trailing edge of the armature contact regions. This wear pattern will be discussed further later, especially with regard to the inconsistencies it provides with the current model.

Figure 2a. Side view of post-transition armature wear pattern. Note preferential corner erosion.

Figure 2b. Nearly isometric view of post-transition armature wear pattern. Note preferential corner erosion.

The results obtained by using R=0.50 mm are shown in table 2. The variation of T, da/dt, the ionization fractions, and the specific internal energy as functions of the armature-rail gap size, R, are presented graphically in figure 3.

Table 2. Results of the transition interface model for R=0.50 mm.

T	74000 K
α_0	0.00019
α_1	0.030
α_2	0.16
α_3	0.80
$\frac{da}{dt}$	0.0011 mm/μs

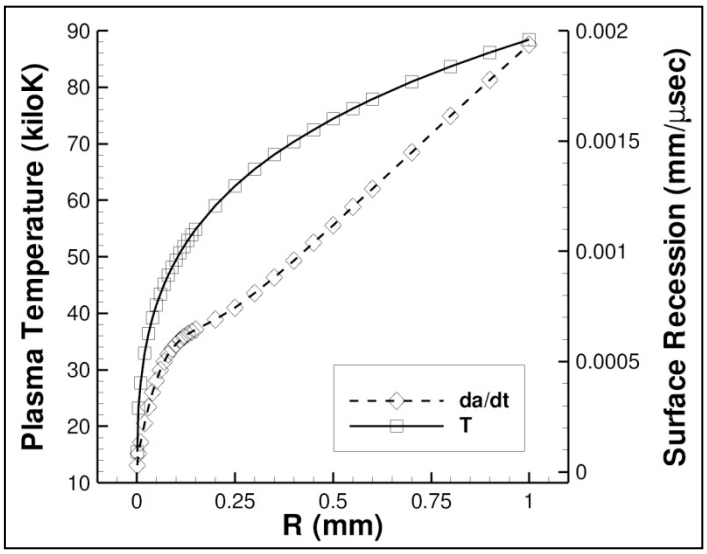

Figure 3a. Variation of plasma temperature and armature recession rate as functions of the gap size.

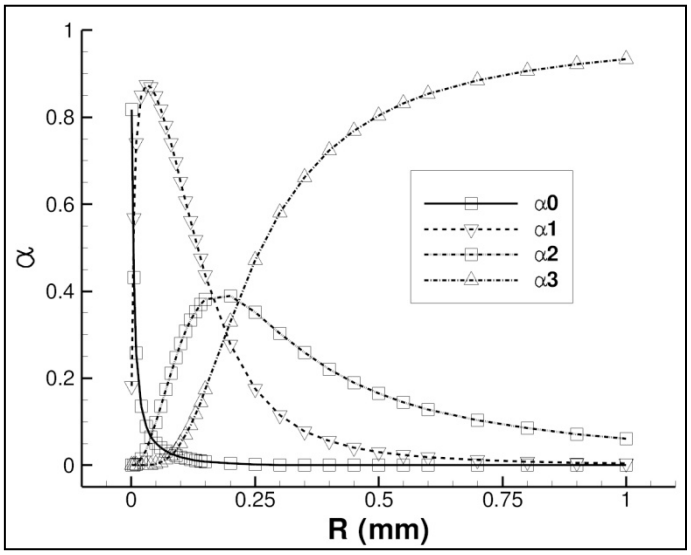

Figure 3b. Variation of ionization fractions as a function of the gap size.

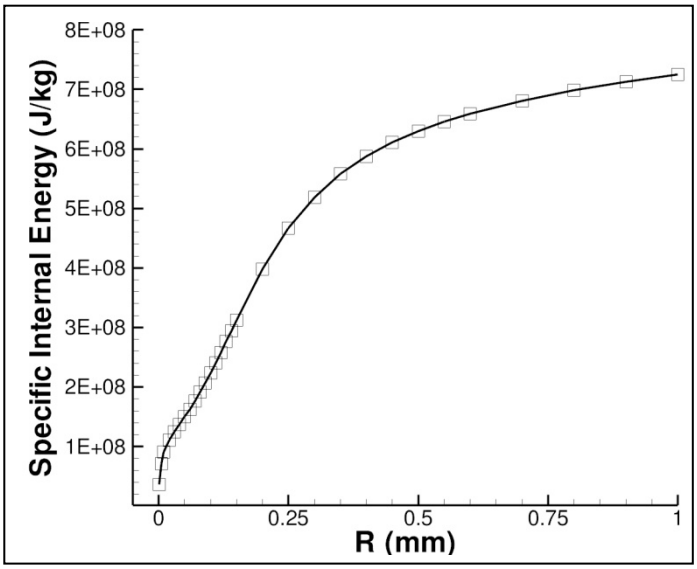

Figure 3c. Variation of the specific internal energy as a function of the gap size.

Visual inspection of post-transition armatures shows that a minimum of 0.5 mm of material must be lost from each rail-facing side of the armature in the post-transition interface. By iterating the surface recession as a function of time, assuming an initial gap spacing of R=0.001 mm, the 0.5 mm gap can be achieved in 875 μs. Typical post-transition transit times for this armature/current configuration are on the order of 1500 μs, thus there is plenty of time for thermal vaporization to remove the necessary amount of material. There are problems with this result, however. The total surface recession and the recession rate for this iterative solution are shown in figure 4. Extracting the recession rate from figure 4 and matching that to a plasma temperature from figure 3a shows that the temperature very quickly exceeds 60000 K. At this temperature, approximately 50% of the vapor is in the third ionized state. When more than half of the vapor is in the highest ionized state modeled, this typically means that higher ionization states must be included. However, the idea that the aluminum plasma in the interface is in the fourth ionized state or higher is unlikely given typical ablation/plasma generation problems never reach this level of ionization. Equally unlikely is the idea that the plasma temperature in the interface can exceed 70000 K. This high temperature poses a serious problem for plasma confinement.

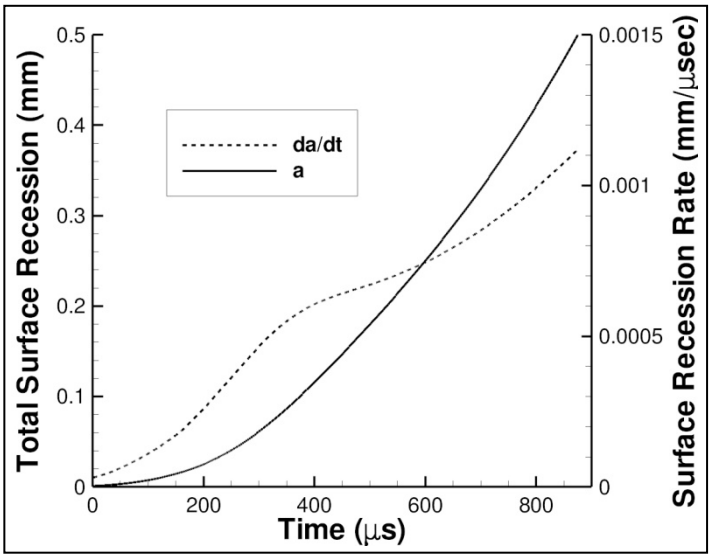

Figure 4. Total surface recession and recession rate as functions of time to generate a 0.5 mm gap.

In the present thermal vaporization mode, the plasma can only be generated in the small region where the electric current is confined. However, visual analysis of transitioned armatures show damage is not confined to a narrow region at the trailing edge of the armature (see figure 2). This implies that the plasma expands outside the generation region, which is logical given the high plasma pressure. However, if the plasma expands, that will significantly decrease the plasma density and temperature (recall that the current carrying region is on the order of a few millimeters). Any decrease in plasma density or temperature will cause a significant decrease in the vaporization rate, as shown in figure 3a. Also, if plasma expansion were happening, one would expect to see uniform damage at the armature-rail contact region. If plasma expanded into a less confined region, then the vaporization rate would decrease. Thus, more uniform wear should result. On the contrary, significant wear is seen at the edges of the armature (at sharp corners).

The implication from the model is that simple thermal vaporization is likely not responsible for the armature damage observed, due to the need for unrealistically high temperature, persistent, unconfined plasma to exist in the interface. Rather, the wear mechanism must generate a much higher surface recession rate at lower temperatures, while also accounting for preferential corner/edge volume loss. The most likely candidate is arcing electrical contact.

4. Requirements for an Arcing Contact Interface Model

As discussed above, simple thermal vaporization cannot explain the pattern of wear seen on recovered transitioned armatures, nor the volume of material lost. A potential solution for both

the non-uniform armature wear pattern and the higher total mass loss is the existence of arcing contact in the post-transition interface.

The fundamentals of arcing electrical contact are best presented elsewhere (Boxman, 1995). The relevant fact here is that arcing solves the two problems presented above. First, arc plasma temperatures can be extremely high, resulting is very large, yet localized, ablation rates. Secondly, electric arcs naturally prefer sharp corners and peaks as discharge locations. This preference for sharp edges will result in preferential corner erosion and help to explain the armature wear patterns seen on recovered transitioned armatures.

If the development of an arcing contact transition interface is pursued, there are unique considerations that must be included that do not appear in any other application. Typically, arc gaps are on the order of a few centimeters or larger. In the armature-rail interface, gap spacings can reach one millimeter, but are likely a few tenths of a millimeter for most of the armature in-bore transit time. Small gap spacings can result in a loss of the definition between the cathode spot, plasma column, and anode spot regions, which may necessitate a drastically different modeling framework than is typically used in arc discharge. Further complicating this phenomenon is the large electrical current that must be accommodated by the arc. Typical arc discharges involve currents in the range of a few milliamps up to tens of kiloamps. Railgun currents are routinely several mega-amps (Powell et al., 2005). This large current means that many models for plasma ionization and thermal conduction in the arc must be modified or replaced altogether. It is unclear what specific physical phenomena are important when this large current is combined with small gap spacing. A considerable effort must be undertaken to investigate this combination of factors if an accurate model of arcing contact in the armature-rail interface is to be pursued. This effort will obviously involve extensive theoretical and computational work, but may necessitate experimental work as well in order to validate computational models or probe any “new physics” that may arise given the combination of small gap spacing and high currents.

5. Conclusion

Presented was a model for the post-transition interface encountered in solid armature railguns under the assumption that the interface is categorized by thermal vaporization of the armature. In the model, the vaporized armature material is thermally ionized and carries the electric current through the armature-rail gap. The model indicates that the vaporization rate is sufficient to account for the total volume of armature material lost in the post-transition environment, however, it fails to explain the pattern of armature wear seen on recovered transitioned armatures. These results indicate that the post-transition interface is likely categorized by arcing contact. The unique challenges presented by arcing contact in the armature-rail interface are discussed briefly to provide a roadmap to future researchers.

6. References

Abrams, M. B.; Tzeng, J. T.; Zielinski, A. E.; Niles, S. *Quantified Erosion of Chromium-Copper and Steel Cladding in a Multishot Railgun Bore*; ARL-TR-4117; U.S. Army Research Laboratory: Aberdeen Proving Ground, MD, May 2007.

Barber, J. P.; Bauer, D. P.; Jamison, K.; Parker, J. V.; Stefani, F.; Zielinski, A. A Survey of Armature Transition Mechanisms. *IEEE Transactions on Magnetics* **January 2003**, *39* (1).

Boxman, R. L. *Handbook of Vacuum Arc Science and Technology*; Noyes Publications, 1995.

Crank, J. *Free and Moving Boundary Problems*; Oxford University Press, 1987.

Marshall, R. A. *The Properties of Copper and Hydrogen Plasmas*, 80 Cliff Rd, Wollongong NSW 25000, Australia, September 1986.

Powell, J. D.; Zielinski, A. E. *Electrodynamics of Rail-Armature Interface in a Solid-Armature Railgun*; ARL-TR-3663; U.S. Army Research Laboratory: Aberdeen Proving Ground, MD November 2005.

Powell, J. D.; Zielinski, A. E. *Theory and Experiment for an Ablating-Capillary Discharge and Application to Electrothermal-Chemical Guns*; BRL-TR-3355; June 1992.

Zielinski, A. E.; Denny, A. *Single-Shot Rail Damage Related to Linear Current Density in a Solid-Armature Railgun*; ARL-TR-4789; U.S. Army Research Laboratory: Aberdeen Proving Ground, MD, April 2009.

NO. OF COPIES	ORGANIZATION
1 ELEC	ADMNSTR DEFNS TECHL INFO CTR ATTN DTIC OCP 8725 JOHN J KINGMAN RD STE 0944 FT BELVOIR VA 22060-6218
1 CD	OFC OF THE SECY OF DEFNS ATTN ODDRE (R&AT) THE PENTAGON WASHINGTON DC 20301-3080
1	US ARMY RSRCH DEV AND ENGRG CMND ARMAMENT RSRCH DEV & ENGRG CTR ARMAMENT ENGRG & TECHNLGY CTR ATTN AMSRD AAR AEF T J MATTS BLDG 305 ABERDEEN PROVING GROUND MD 21005-5001
1	PM TIMS, PROFILER (MMS-P) AN/TMQ-52 ATTN B GRIFFIES BUILDING 563 FT MONMOUTH NJ 07703
1	US ARMY INFO SYS ENGRG CMND ATTN AMSEL IE TD A RIVERA FT HUACHUCA AZ 85613-5300
1	COMMANDER US ARMY RDECOM ATTN AMSRD AMR W C MCCORKLE 5400 FOWLER RD REDSTONE ARSENAL AL 35898-5000
1	US GOVERNMENT PRINT OFF DEPOSITORY RECEIVING SECTION ATTN MAIL STOP IDAD J TATE 732 NORTH CAPITOL ST NW WASHINGTON DC 20402
1	UNIV AT BUFFALO-SUNY/AB ATTN J SARJEANT 312 BONNER-ELECT ENGR PO BOX 601900 BUFFALO NY 14260-1900

NO. OF COPIES	ORGANIZATION
1	UNIV OF TEXAS AT AUSTIN ATTN ENS 434 DEPT OF ECE M DRIGA MAIL STOP 60803 AUSTIN TX 78712
2	UNIV OF TEXAS AT AUSTIN CTR FOR ELECT ATTN J KITZMILLER ATTN J PAPPAS PRC MAIL CODE R7000 AUSTIN TX 78712
5	UNIV OF TEXAS AT AUSTIN INST FOR ADVNCED TECH ATTN F STEPHANI ATTN I MCNAB ATTN K T HSIEH ATTN S SATAPATHY ATTN T WATT 3925 WEST BRAKER LN STE 400 AUSTIN TX 78759-5316
2	BAE ATTN MS M170 R JOHNSON ATTN MS M401 B GOODELL 4800 E RIVER RD MINNEAPOLIS MN 55421-1498
2	IAP RSRCH INC ATTN D BAUER ATTN J BARBER 2763 CULVER AVE DAYTON OH 45429-3723
1	SAIC ATTN J BATTEH 4901 OLDE TOWNE PKY STE 200 MARIETTA GA 30068
1	SAIC ATTN K JAMISON PO BOX 4216 FT WALTON BEACH FL 32542
1	SAIC ATTN A WALLS 8303 N MOPAC EXPY STE B 450 AUSTIN TX 78759

NO. OF COPIES	ORGANIZATION
3	US ARMY RSRCH LAB ATTN RDRL WM P PLOSTINS ATTN RDRL WML D A ZIELINSKI ATTN RDRL WML G A MICHLIN ABERDEEN PROVING GROUND MD 21005
1	US ARMY RSRCH LAB ATTN RDRL WML H C CANDLAND BLDG 4600 ABERDEEN PROVING GROUND MD 21005
2	US ARMY RSRCH LAB ATTN RDRL WMM A J TZENG ATTN RDRL WMM A R EMERSON ABERDEEN PROVING GROUND MD 21005
1	US ARMY RSRCH LAB ATTN RDRL WMM B R P KASTE BLDG 4600 ABERDEEN PROVING GROUND MD 21005
5	US ARMY RSRCH LAB ATTN RDRL WMP A A PORWITZKY (4 COPIES) ATTN RDRL WMP A B RINGERS ABERDEEN PROVING GROUND MD 21005
1	US ARMY RSRCH LAB ATTN RDRL WMP A J POWELL BLDG 1116A ABERDEEN PROVING GROUND MD 21005
1	US ARMY RSRCH LAB ATTN RDRL WMP A W UHLIG ABERDEEN PROVING GROUND MD 21005
1	US ARMY RSRCH LAB ATTN RDRL CIM G T LANDFRIED BLDG 4600 ABERDEEN PROVING GROUND MD 21005-5066

NO. OF COPIES	ORGANIZATION
1	US ARMY RSRCH LAB ATTN RDRL WML D M DEL GUERCIO ABERDEEN PROVING GROUND MD 21005-5066
1	US ARMY RSRCH LAB ATTN RDRL WMP A C HUMMER BLDG 1116A ABERDEEN PROVING GROUND MD 21005-5066
3	US ARMY RSRCH LAB ATTN IMNE ALC HRR MAIL & RECORDS MGMT ATTN RDRL CIM L TECHL LIB ATTN RDRL CIM P TECHL PUB ADELPHI MD 20783-1197

TOTAL: 43 (1 ELEC, 1 CD, 41 HCS)

INTENTIONALLY LEFT BLANK.